

## Phonoconductivity measurement of the phonon absorption by a two-dimensional hole gas in a GaAs heterojunction

A. J. Kent, R. E. Strickland, K. R. Strickland, and M. Henini

*Department of Physics, University of Nottingham, University Park, Nottingham NG7 2RD, United Kingdom*

(Received 30 January 1996)

In this paper we describe measurements of the absorption of acoustic phonons from a ballistic heat pulse by a two-dimensional (2D) hole gas in a GaAs/Al<sub>x</sub>Ga<sub>1-x</sub>As heterojunction. The phonoconductivity technique was used, in which the change in the resistance of a device caused by phonon absorption is detected. Direct information regarding the hole-phonon interaction in a heterojunction is obtained by this method. Measurements of the phonoconductivity in zero and quantizing magnetic fields were made and compared with the results of numerical calculations of the absorption. In spite of the complicated nature of the 2D hole subbands and the hole-phonon coupling, we find that, at the hole densities and temperatures of these experiments, the theory describing the interaction of 2D electrons with phonons can be reasonably applied to 2D holes with the appropriate change of the effective mass and other relevant parameters, and the use of a single effective valence-band deformation potential. Using our results, we are able to determine the Fang-Howard parameter for the confined holes and the effective mass for heavy holes in the spin-split lowest subband. [S0163-1829(96)05227-7]

### I. INTRODUCTION

Phonon spectroscopy is a powerful technique for the study of two-dimensional carrier gases (2DCG's) in semiconductors (for a review, see Ref. 1). The wavelength of acoustic phonons is comparable to the important length scales in the system such as the Fermi wavelength and the thickness of the 2D gas. Furthermore, phonons couple effectively to the carrier system via the deformation potential and piezoelectric interaction (the latter is only effective in crystals without a center of inversion symmetry such as GaAs). It is also important to understand the details of the carrier-phonon interaction because of its effect on device parameters. Hot carriers relax by phonon emission, and phonon-scattering limits the mobility of 2D carriers at normal temperatures. Direct phonon measurements are a better way to obtain this kind of information because the details regarding the magnitude, direction, and polarization of the phonon wave-vector are preserved. The phonoconductivity technique has been used to study 2D electron gases in silicon metal oxide semiconductor field-effect transistors and GaAs heterojunctions in zero and quantizing magnetic fields.<sup>2-4</sup> Information regarding the nature of the electron states and the phonon scattering processes has been obtained in these experiments.

To date there have been few direct phonon measurements on 2D hole systems, except for some experiments on the phonon emission by electrically heated holes in *p*-type multiple quantum wells and heterojunctions.<sup>5,6</sup> In those experiments a short  $\approx 20$ -ns heating pulse was applied to the device, and the emitted phonons were detected using a superconducting bolometer on the opposite face of the substrate. Using this technique it was possible to resolve the different phonon modes that are emitted. The results showed a tenfold increase in the energy relaxation rate due to acoustic-phonon emission compared with a 2D electron gas

at the same carrier temperature.<sup>7</sup> This difference can be mostly accounted for by the difference in effective mass between electrons and holes. It is also consistent with the observation that the mobility of 2D holes in high-quality modulation-doped *p*-type heterojunctions continues to increase as the temperature is reduced to below 4 K.<sup>8</sup> In *n*-type samples the temperature dependence of the mobility is very weak below about 4 K. Another feature apparent in phonon emission experiments is the strong coupling to longitudinal acoustic (LA) modes. With the *p*-type systems a strong LA mode signal is seen, whereas in the case of electrons the transverse mode is totally dominant. It is possible that this difference is due to a stronger vertical confinement for the holes in a heterojunction owing to their higher effective mass.

Rigorous theoretical calculations of the interaction of phonons with 2D holes are generally more difficult than in the case of electrons owing to the rather complicated hole subband structure in heterojunctions.<sup>9</sup> However, at low temperatures and low hole density only the bottom two subbands are occupied. Close to  $k_{\parallel}=0$  the bands are approximately parabolic, and so the calculations used for 2D electrons, with appropriate changes to certain parameters such as the effective mass and the thickness of the 2D layer, may be applicable. This approach has been shown to work adequately in calculations of the phonon-limited mobility of 2D holes,<sup>10</sup> where detailed information regarding the mode and angular dependence of the phonon coupling is not required. There is also some evidence provided by the emission experiments to suggest that this simplified approach may be able to account for some observations in direct phonon experiments, but more experimental data are required for verification.

In zero applied magnetic field the phonoconductivity response of an *n*-type heterojunction is rather weak. Owing to the apparently stronger coupling of acoustic phonons with 2D holes than with 2D electrons, we would expect a two-dimensional hole gas (2DHG) to be a better candidate for study by the phonoconductivity technique. In this paper we

describe the first phonoconductivity experiments on a 2D hole gas in a gated (100) GaAs/Al<sub>x</sub>Ga<sub>1-x</sub>As heterojunction.

## II. THEORY

### A. 2D hole band structure

The band structure of 2D holes in a modulation-doped heterostructure has been calculated by a number of authors.<sup>9,11</sup> It turns out to be rather complicated with the bands being somewhat rather distorted and anisotropic. At  $k_{\parallel}=0$ , the lowest two subbands are separated by about 15 meV, which means at liquid-helium temperatures and typical carrier densities  $<1 \times 10^{16}/\text{m}^{-2}$ , only the lowest (heavy hole, HH1) band is occupied. However, owing to the strong spin-orbit interaction in GaAs and the asymmetric nature of the confining potential in heterostructures, the Kramers degeneracy of this band is lifted for  $k_{\parallel} \neq 0$ . So it splits into two bands, the so called ‘‘heavy-hole’’ band with spin = +3/2, and the ‘‘light-hole’’ band with spin = -3/2.

The effective masses in the two bands have also been calculated in Refs. 9 and 11, the zero-field values of the heavy hole mass,  $m_{h+}^*/m_0$ , were found to be 0.44 and 0.46, respectively, and the corresponding light-hole masses  $m_{h-}^*/m_0$ , were 0.17 and 0.12. Cyclotron resonance measurements<sup>12</sup> gave heavy- and light-hole masses of 0.60 and 0.38, respectively, while Shubnikov–de Haas data<sup>13</sup> yields extrapolated zero-field values of 0.09–0.35 for the light-hole mass and 0.24–0.59 for the heavy-hole mass, depending on carrier density. It has also been found that the proportion of holes in the lowest (heavy) hole subband is between 61% (Ref. 12) and 73%,<sup>13</sup> again depending on the overall density.

The phonon interaction with a 2DCG is dependent on the effective mass, being enhanced at higher mass, and so, taking account of the difference in population of the two bands as well, it seems reasonable to assume that the heavy-hole subband will dominate the phonoconductivity response.

An added complication when considering  $p$ -type systems is the nature of the deformation potential coupling in the valance band. Whereas in the conduction band of GaAs there is a single deformation potential, in the valance band there are three independent constants.<sup>14,15</sup> It has been found that it is sufficient to use an ‘‘effective’’ deformation potential<sup>16</sup> in order to account for the transport properties in  $p$ -type GaAs, we will use the same approximation in the theory that follows.

### B. Theory of phonon absorption by a 2DHG

The formal theory of the absorption of phonons by a 2D electron gas in a silicon inversion layer was calculated by Hensel and co-workers.<sup>17,18</sup> In the theory which follows we will make the *a priori* assumption that under the conditions relevant to this work, the 2DHG in GaAs can be treated in the same way except for the appropriate changes to the material parameters and carrier effective masses. We believe that this assumption is reasonable because close to  $k_{\parallel}=0$ , the heavy-hole band is approximately parabolic and also isotropic in the plane.

Consider the situation in which a beam of phonons of wave vector  $q$  are incident on a 2D hole gas at temperature

$T_h$ . It is assumed that the 2DHG and lattice are in thermal equilibrium, i.e.,  $T_h = T_l$ , and the absorption is sufficiently weak that  $T_h$  is not raised significantly. The incident phonons produce an excess population  $\Delta n_q$  in phonon mode  $q$  such that the net phonon distribution in the region of the 2DHG is given by

$$n_q = n_q(T_h) + \Delta n_q.$$

The net power incident on the 2DHG due to this mode is given by

$$P_{\text{inc}} = \hbar \omega \nu_s \cos(\theta) A \left( \frac{\Delta n_q}{V} \right),$$

where  $\nu_s$  is the group velocity of the phonon,  $\theta$  the angle of incidence of the beam relative to the normal to the 2DHG,  $A$  the active area of the 2DHG, and  $V$  the sample volume. The rate of energy absorption from the mode due to the hole-phonon interaction is given by

$$R_{\text{abs}} = -\hbar \omega \frac{dn_q}{dt}.$$

Hence the fractional absorption from the incident phonon beam is

$$\alpha = \frac{R_{\text{abs}}}{P_{\text{inc}}} = -\frac{V}{A \nu_s \cos \theta} \frac{1}{\Delta n_q} \frac{dn_q}{dt},$$

where the change in the phonon occupation number is given by (from the Fermi golden rule)

$$\frac{dn_q}{dt} = \sum_k f_k (1 - f_{k'}) (n_q + 1) W_k^{k',q} - f_{k'} (1 - f_k) n_q W_{k'}^k.$$

Here  $f_k$  are the hole distribution functions at  $T_h$ ;  $k$  and  $k'$ , respectively, refer to the initial and final carrier states; the two terms on the right correspond to phonon emission and absorption processes respectively, with transition probabilities  $W_k^{k',q}$  and  $W_{k'}^k$ ,

$$W_k^{k',q} = W_{k'}^k = \frac{2\pi}{\hbar} |M_k^{k',q}|^2 \delta(E_k - E_{k'} - \hbar \omega_q),$$

where  $M_k^{k',q} = \langle k' | V_{e-p} | k \rangle$  is the transition matrix element.

In gallium arsenide, acoustic phonons couple to carriers via the deformation potential and piezoelectric interaction. In contrast to the case of a two-dimensional electron gas in GaAs, both longitudinal and transverse modes couple to 2D holes via the deformation potential.<sup>15</sup> For deformation-potential interaction (ignoring screening),

$$|M_k^{k',q}|^2 = \frac{\hbar \Xi_{\nu}^2 q}{2\rho V \nu_s} |F(q_{\perp})|^2 \delta_{k,k'+q_{\parallel}},$$

for the piezoelectric interaction coupling to longitudinal acoustic (LA) modes,

$$|M_k^{k',q}|^2 = \left( \frac{eh_{14}}{\epsilon \epsilon_q} \right)^2 \frac{9q_{\parallel}^4 q_{\perp}^2}{2q^7} \frac{\hbar}{2\rho V \nu_{sL}} |F(q_{\perp})|^2 \delta_{k,k'+q_{\parallel}},$$

and for the piezoelectric interaction coupling to transverse acoustic (TA) modes,

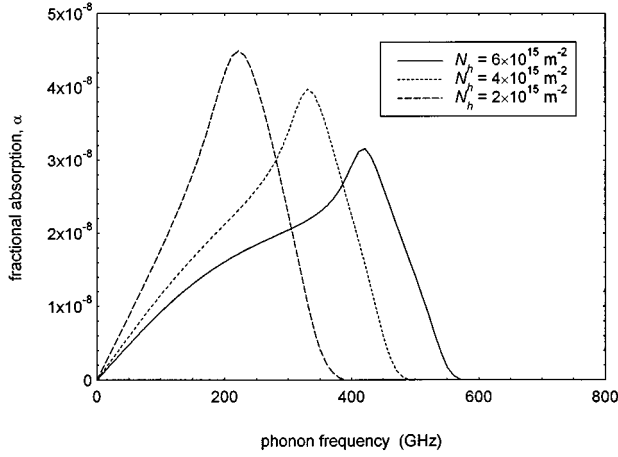


FIG. 1. Fractional absorption as a function of phonon frequency for  $\theta=45^\circ$ ,  $a_0=1$  nm, and at three values of  $N_h$ .

$$|M_k^{k',q}|^2 = \left( \frac{eh_{14}}{\epsilon\epsilon_q} \right)^2 \frac{8q_{\parallel}^4 q_{\perp}^2 + q_{\parallel}^6}{2q^7} \frac{\hbar}{2\rho V v_{sT}} |F(q_{\perp})|^2 \delta_{k,k'+q_{\parallel}},$$

where  $\Xi_v$  is the effective deformation potential constant for the valence band,  $h_{14}$  is the piezoelectric coupling constant,  $\epsilon$  is the dielectric constant,  $\epsilon_q$  the screening parameter,  $\rho$  the crystal density, and  $V$  the normalizing volume. The term  $\delta_{k,k'+q_{\parallel}}$  represents in-plane momentum conservation, and the form factor  $|F(q_{\perp})|^2$  accounts for momentum conservation perpendicular to the plane of the carrier gas. For a triangular confining potential,

$$|F(q_{\perp})|^2 = \frac{1}{(1+q_{\perp}^2 a_0^2)^3},$$

where  $a_0$  is the Fang-Howard parameter, and is related to the ‘width’ of the 2D gas.<sup>19</sup>

### C. Numerical results

We are now in a position to calculate some features of the phonon absorption numerically, at this stage we are ignoring screening and the effects of acoustic anisotropy in the GaAs substrate. The latter can be introduced at a later stage when the angular distribution of wave vectors is known. In the results that follow, we have assumed  $m^*/m_0=0.4$ ,  $\Xi_v=4.9$  eV,<sup>20</sup>  $h_{14}=1.2 \times 10^9$  V m<sup>-1</sup>,<sup>21</sup>  $T_s=1.5$  K,  $v_{sL}=5500$  ms<sup>-1</sup>,  $v_{sT}=3300$  ms<sup>-1</sup>, and  $\epsilon=12.9$ .<sup>21</sup>

The dependence of the fractional absorption,  $\alpha$ , on phonon frequency for deformation potential coupled LA modes at  $\theta=45^\circ$  and for  $a_0=1$  nm is shown in Fig. 1. This clearly shows the effect of the so-called  $2k_F$  cutoff; i.e., when  $q_{\parallel} [= (\omega/v_s)\sin 45]$  exceeds  $2k_F$ , absorption is prevented by the in-plane momentum conservation condition. The cutoff is seen to shift to lower frequencies as  $N_h$ , hence  $k_F$ , is reduced. In Fig. 2 is shown the dependence of  $\alpha$  on phonon frequency at nearer to normal incidence,  $\theta=10^\circ$ , with  $N_h=3 \times 10^{15}$  m<sup>-2</sup> and also for deformation-potential coupling. At this angle, the in-plane momentum component is small and the reduction of absorption at high frequencies is

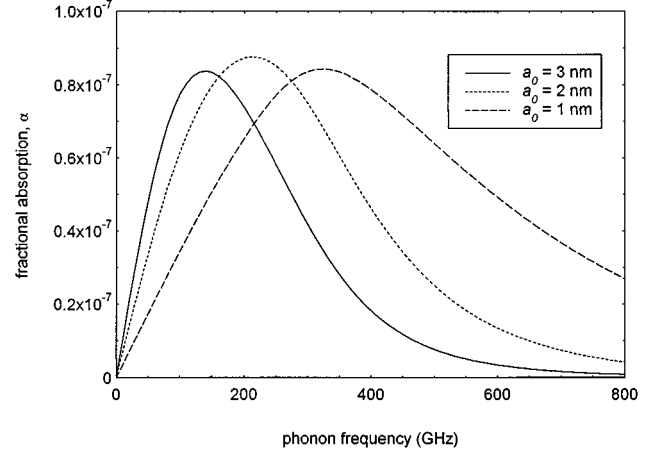


FIG. 2. Fractional absorption as a function of phonon frequency for  $\theta=10^\circ$ ,  $N_h=3 \times 10^{15}$  m<sup>-2</sup>, and for three values of  $a_0$ .

now due to the effect of the form factor  $|F(q_{\perp})|^2$ . The high-frequency rolloff is more severe for larger values of  $a_0$  (thicker 2DHG).

Figure 3 shows the dependence of  $\alpha$  on the incidence angle of the phonons for deformation-potential coupling, this time for a phonon source with a broadband (Planckian) spectrum, i.e.,  $\Delta n_q(\omega) \propto \omega^2 / \{\exp(\hbar\omega/kT_s) - 1\}$ , where  $T_s$  is the phonon source temperature. In this case  $N_h=3 \times 10^{15}$  m<sup>-2</sup>,  $a_0=1$  nm, and  $T_s=15$  K. The fractional absorption is rather small, at most about  $4 \times 10^{-6}\%$ . This figure is broadly consistent with that estimated from experimental measurements on silicon two-dimensional electron-gas (2DEG) devices<sup>2</sup> for which the relevant parameters: deformation potential constant,  $m^*$ ,  $a_0$ , etc. are similar. The reduction of the absorption at large angles is due to the  $2k_F$  cutoff. The cutoff is more severe for the TA mode owing to its larger wave vector corresponding to the same frequency. The absorption is also very effectively cutoff at small angles,  $\theta = \sin^{-1}(v_s/v_F)$ .

It was found that, even when screening is ignored, the fractional absorption due to piezoelectric coupling was some 2–3 orders of magnitude weaker than for deformation-potential coupling, and so can be ignored for the purposes of this work. The effect of including screening would probably

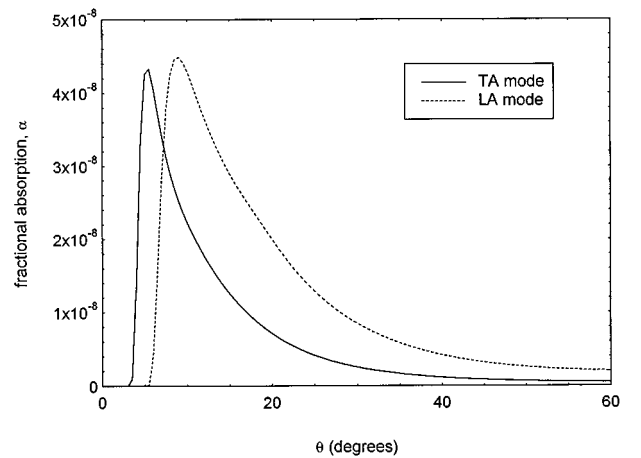


FIG. 3. Angular dependence of the fractional absorption for a Planckian source with  $T_s=15$  K,  $N_h=3 \times 10^{15}$  m<sup>-2</sup>, and  $a_0=1$  nm.

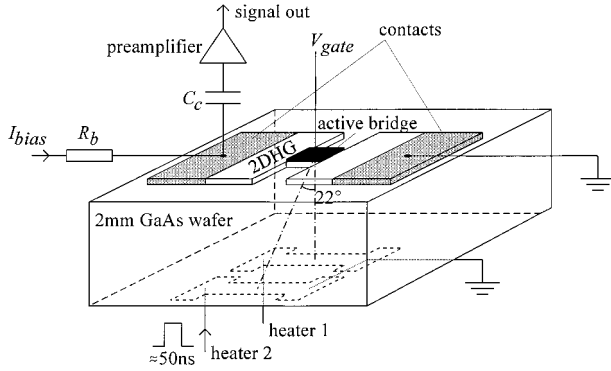


FIG. 4. Experimental arrangement for phonoconductivity measurements. Not shown in the picture is one further heater at  $31^\circ$  to the device normal.

be to further shift the balance in favor of the short-range deformation potential coupling.

#### D. Absorption in a magnetic field applied normal to the 2DHG

If a magnetic field  $\mathbf{B}$  is applied normal to the plane of the 2DHG its energy spectrum breaks up into a series of Landau levels for  $\mu B > 1$ . The interaction of phonons with a 2DEG in an applied magnetic field has been considered for the case of very sharp Landau levels,<sup>22</sup> and the more realistic case of Landau levels broadened by disorder.<sup>23,24</sup> Although these papers were concerned with the process of phonon emission, details of the interaction are common to both emission and absorption. Making use of the assumptions in Sec. II B above, their results can also be applied to the case of a 2DHG to obtain the main features of the absorption in a magnetic field. There turn out to be two kinds of absorption process possible: Cyclotron phonon absorption, which is associated with hole transitions between Landau levels, and low-frequency phonon absorption accompanied by intra-Landau-level transitions. The probability of the former is a maximum when  $E_F$  is midway between two Landau levels, and for the latter it is a maximum when  $E_F$  is coincident with a Landau level. The in-plane momentum conservation rule changes from  $q_{\parallel} \leq 2k_F$  to  $q_{\parallel} \leq l_B^{-1}$ , where  $l_B$  is the magnetic length, while the form-factor-imposed restriction on the perpendicular momentum component remains the same.

### III. EXPERIMENTAL DETAILS

The samples used in these studies were based on two molecular-beam epitaxy (MBE)-grown (001) GaAs/ $\text{Al}_x\text{Ga}_{1-x}\text{As}$   $p$ -type heterojunctions: NU900, which was grown on a 2-mm-thick semi-insulating GaAs wafer, and NU899, grown on a standard 0.4-mm substrate. The layer structure was identical for both and consisted of a superlattice,  $50 \times (25\text{-}\text{\AA} \text{ GaAs}/25\text{-}\text{\AA} \text{ Al}_x\text{Ga}_{1-x}\text{As})$ ; a  $0.5\text{-}\mu\text{m}$  GaAs buffer; a  $205\text{-}\text{\AA}$   $\text{Al}_x\text{Ga}_{1-x}\text{As}$  spacer;  $408\text{-}\text{\AA}$   $\text{Al}_x\text{Ga}_{1-x}\text{As}$ , Be doped to  $1.3 \times 10^{18} \text{ m}^{-2}$ ; and a  $170\text{-}\text{\AA}$  GaAs cap. At 1 K the 2D hole density was  $3.3 \times 10^{15} \text{ m}^{-2}$ , and the mobility  $5 \text{ m}^2/\text{V}^{-1} \text{ s}^{-1}$ .

The sample arrangement is shown in Fig. 4. The 2DHG device was defined by an etch, and consisted of a narrow

bridge  $120 \mu\text{m}$  long by  $50 \mu\text{m}$  wide, with a pair of large-area,  $1\text{-mm}^2$ ,  $p$ -type (AuZnAu) contacts formed at its ends. The large contact area was considered necessary to reduce the contact resistance relative to the channel, and so minimize any possible spurious responses from the contacts. To further reduce contact effects, the diffused contacts were also spatially removed from the active bridge by wider areas of 2DHG. With this arrangement,  $>90\%$  of the measured device resistance was due to the narrow bridge. A TiAu gate was fabricated above the bridge and was used to control the hole areal density. The opposite side of the GaAs wafer was polished and a  $600 \times 60\text{-}\mu\text{m}^2$  CuNi heater deposited by vacuum evaporation, its thickness was about 70 nm, giving the heater a resistance of  $50 \Omega$ . The sample was mounted in an optical-access cryomagnetic system in which it could be held at temperatures down to 1.3 K under pumped liquid helium, and magnetic fields of 0–7 T could be applied perpendicular to the plane of the 2DHG. Subminiature low-loss coaxial cables were used to connect the device and heater to the instrumentation outside the cryostat.

The device was characterized at a temperature of 1.5 K by means of Shubnikov–de Haas measurements. At zero gate bias the 2DHG density  $N_h$  was  $3.3 \times 10^{15} \text{ m}^{-2}$ , this was seen to decrease with increasing positive gate bias  $V_G$ , and by applying a suitably high bias it was possible to fully deplete the channel. However, it was noticed that for  $N_h \leq 1.5 \times 10^{15} \text{ m}^{-2}$  the mobility began to drop rapidly. Applying a negative gate bias caused a slight enhancement of the hole concentration. The gate leakage current was less than  $1 \mu\text{A}$  for  $V_G \leq +2 \text{ V}$ . The two-terminal resistance of the device increased with temperature in the range 1.5–4.2 K. Unlike in the case of an  $n$ -type device, there is still a significant temperature dependence at the lowest temperatures in this range. For  $N_h = 3.3 \times 10^{15} \text{ m}^{-2}$ , the temperature coefficient of the resistance was about  $220 \Omega \text{ K}^{-1}$  at 1.5 K.

By applying a short (typically 10–50 ns) current pulse to the heater, a burst of nonequilibrium phonons could be injected into the GaAs substrate. The phonon spectrum is approximately Planckian with a peak at  $\omega_{\text{dom}} \approx 3kT_s/\hbar$ , and the heater temperature  $T_s$  can be deduced using acoustic mismatch theory.<sup>25</sup> For a CuNi heater on GaAs,

$$P_h/A \approx 524(T_s^4 - T_l^4),$$

where  $P_h$  is the electrical power supplied to the heater,  $A$  the heater area, and  $T_l$  the substrate (lattice) temperature. In these experiments  $T_l = 1.5 \text{ K}$ . Typically  $T_s$  is in the range 5–15 K, and at these temperatures the phonons travel ballistically through the substrate at the speed of sound. When the phonons are incident on the 2DHG, absorption leads to a slight change in the device conductance, which is detected as a voltage pulse when a small bias current is applied. The voltage pulse is captured by a fast digitizer and signal averager or a boxcar integrator.

In an alternative arrangement, a continuous film of CuNi was deposited on the back face of the substrate, and phonons were generated at a point by thermalizing in the film pulses from a  $Q$ -switched Nd-YAG (yttrium aluminum garnet) laser. Using this latter arrangement the phonon source is made movable relative to the device by scanning the focused laser spot over the film, and an image of the phonoconductivity

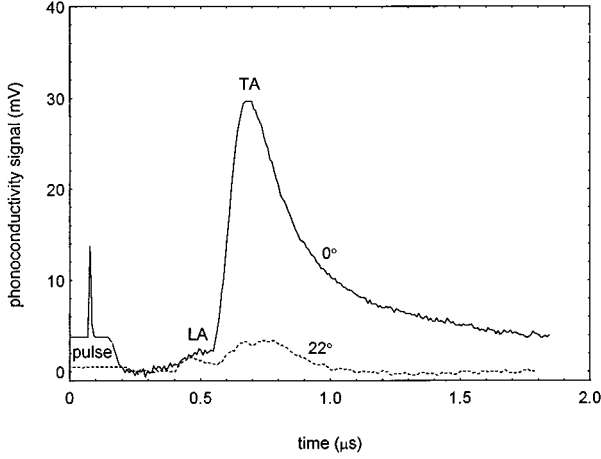


FIG. 5. Phonoconductivity signals obtained using the heater directly opposite the active region of the device and the heater at  $22^\circ$ .

signal is obtained. Such an image directly gives information regarding the angular dependence of the 2DHG-phonon interaction.<sup>26</sup>

#### IV. EXPERIMENTAL RESULTS AND DISCUSSION

In the discussion which follows we assume that the mechanism of detection of phonons by the 2DHG is as follows: The holes absorb energy from the incident phonon beam due to hole-phonon interactions as discussed in Sec. II. This energy is rapidly distributed among the holes by fast hole-hole scattering, leading to a small temperature increase in the 2DHG. The size of the temperature increase,  $\Delta T_h$ , is determined by the balance of the rate of energy absorption from the nonequilibrium phonon beam, and the rate of emission by the heated holes. The dependence of the device resistance on  $T_h$  leads to a small voltage signal being detected when a bias current is passed through the device.

##### A. No applied magnetic field

In Fig. 5 are shown examples of the heat-pulse signals detected by the device, for the heater directly opposite the bridge and at  $22^\circ$  to the normal to the bridge. In both cases  $N_h = 3.3 \times 10^{15} \text{ m}^{-2}$ ,  $T_l = 1.5 \text{ K}$ ,  $P_s = 300 \text{ mW}$  ( $T_s = 11 \text{ K}$ ), and the device bias current was  $100 \mu\text{A}$ . For the source directly opposite the detector, the TA mode clearly dominates. The reason for this is that TA modes are strongly focused close to  $[001]$  in GaAs, and LA modes are slightly defocused in this direction. Taking account of the actual size of the source and detector, the expected TA:LA ratio due to phonon focusing alone is determined using a Monte Carlo simulation program<sup>27</sup> to be 14:1. The measured ratio is actually 14:1, which implies that the strengths of TA and LA absorption within the range of angles covered by the source/detector combination are equal. This is consistent with the theoretical predictions in Fig. 3. At  $22^\circ$  the measured ratio TA:LA is 1.5:1. In this direction the TA:LA focusing ratio is 3:1, which means that the fractional absorption of the TA mode is about half that for the LA mode. This is also consistent with the predictions of the theory.

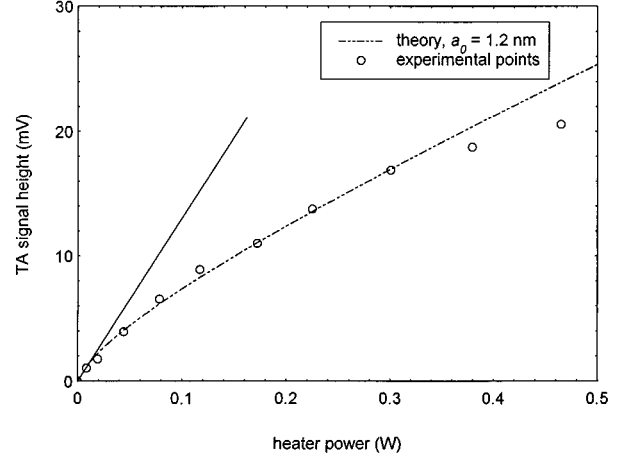


FIG. 6. TA mode signal height as a function of heater excitation power. The solid line indicates a bolometric response, and the broken line is a fit of the theory in Sec. II to the experimental points.

The height of the  $0^\circ$  TA signal in Fig. 5 is 28 mV, taking into account the voltage gain of the amplifiers which is equal to  $625\times$ , this gives a value of  $0.48\Omega$  for the transient change in resistance of the device when the phonons are incident. Using our resistance-temperature calibration, this is found to be equivalent to a hole temperature change  $\Delta T_h$  of just 2.2 mK. It is possible to use this figure to obtain an estimate of the fractional absorption of the hole gas to compare with theory: In equilibrium,

$$P_s f \alpha = N_h A 10^{-16} (T_h^5 - T_l^5),$$

where the left-hand side is the rate of energy absorption by the 2DHG, and the right-hand side the rate of emission determined from our earlier phonon emission measurements.<sup>7</sup> The fraction of the source flux that actually falls on the device,  $f$ , is determined by the sample geometry and phonon focusing effects. In this case  $f = 9 \times 10^{-3}$ , giving  $\alpha \approx 4 \times 10^{-8}$ , which is in remarkable agreement with the theoretical value in Fig. 3.

Although the sample was immersed in superfluid helium, there exists the possibility that, instead of the mechanism described above, a small fraction of the incident phonon energy was being thermalized at the top surface of the wafer and the 2DHG heated by proximity. If this were the case the response is expected to be bolometric, i.e., the signal size should be directly proportional to the power emitted by the heater, as long as this is not so large that phonon scattering in the substrate or nonlinearity in the device resistance-temperature characteristic become significant. Figure 6 shows the TA mode signal height as a function of the power supplied to the heater directly opposite the device bridge. The response is clearly *not* bolometric (indicated by the solid line); it deviates from such behavior at powers well below 0.3 W, at which scattering in the 2-mm GaAs substrate starts to cut in. The reason for the deviation from bolometric behavior is the high-frequency cutoff imposed by the form factor. For near-normally incident phonons this restricts the absorption of phonons with  $q = \omega/v_s > 1/a_0$ . The broken line in Fig. 6 is a fit of the theory to the data points using just two adjustable parameters: A simple scaling factor, which ac-

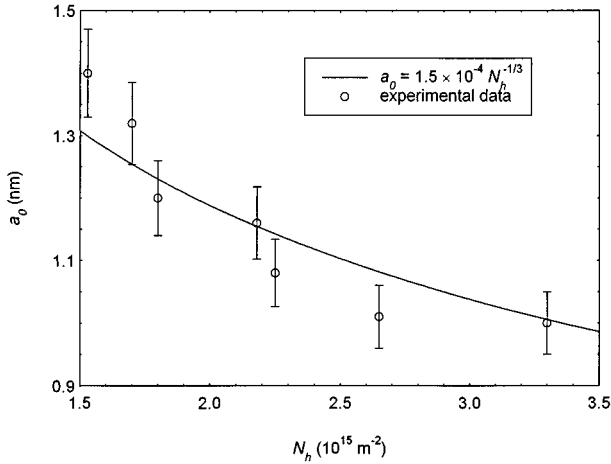


FIG. 7. Values of the Fang-Howard parameter  $a_0$  obtained by fitting the theory to the data obtained at different gate biases and plotted as a function of  $N_h$ .

counts for the sensitivity of the system but does not affect the shape of the curve, and  $a_0$ . The best fit to this set of data was obtained using  $a_0 = 1.2$  nm. The deviation of the data from the fitted curve at  $P_h > 0.3$  W is probably due to phonon scattering in the substrate, measurements on the same wafer material using a conventional superconducting bolometer confirm this. We were also able to fit the theory to data sets obtained at other gate biases and so generate a graph showing how  $a_0$  varies with hole density: Fig. 7. The weak decrease in  $a_0$  with increasing  $N_h$  agrees reasonably with some theoretical calculations, i.e.,<sup>10</sup> (solid line), at all except at the lowest hole densities, where the signals became rather noisy and it was difficult to obtain an accurate determination of  $a_0$ .

For a source at a larger angle the in-plane  $2k_F$  cutoff becomes important. Figure 8 shows the absorption signal as a function of source power for a heater at  $31^\circ$ . At this angle  $q_{\parallel} \approx 0.5\omega_q/\nu_s$ . Like in the case of the  $0^\circ$  heater, the signals deviate strongly from bolometric behavior, owing to suppression of the absorption of high-frequency modes. It is interesting to note that at low powers the ratio of the mode heights LA:TA  $\rightarrow 1$ , whereas at high powers it is about 2.

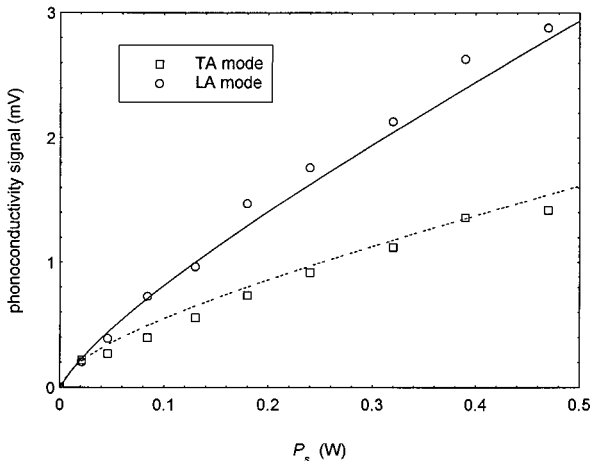


FIG. 8. Experimental (points) and theoretical (lines) TA and LA mode signal heights as a function of excitation power for a heater at  $31^\circ$ .

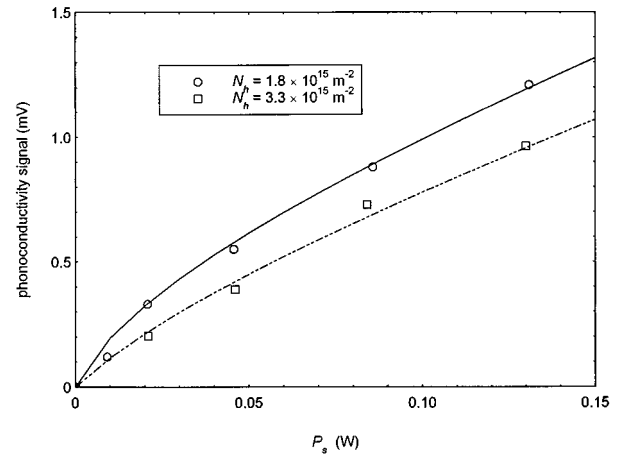


FIG. 9. LA mode signal height as a function of heater power at two different values of 2DHG density. The lines through the data are from the theory.

This means that absorption of the TA mode is more strongly suppressed with increasing power (incident phonon frequency). This behavior is to be expected since, owing to their smaller velocity, TA phonons have a larger wave vector than LA phonons of the same frequency. The lines through the data were obtained using the theory of Sec. II; the only adjustable parameter in this case was the scaling factor which is the same for both curves. This provides further evidence that the simple model of the 2D carrier-phonon interaction we used is quite adequate to describe the experimental results. The effect on the LA-mode absorption of changing the hole density is shown in Fig. 9. The absorption is actually slightly stronger at the reduced hole density, whereas one might naïvely expect the absorption to be weaker at lower density. This must be true of the total absorption integrated over all directions, because the reduction in  $N_h$ , hence  $k_F$ , means the interaction is effectively cut off at smaller angles. However, when we look in a particular direction, as in this experiment, the change in  $\alpha$  may not be very large or even in the opposite direction at certain phonon frequencies; see Fig. 1. Furthermore,  $\alpha$  is also proportional to the thickness of the hole gas, which increases as the density is reduced, so compensating for the reduction in  $N_h$ .

Using the laser heat source we have produced a full image of the phonon absorption: Fig. 10. The image covers an area of  $4 \times 4$  mm<sup>2</sup>, and the boxcar gate was set to capture all modes. The device is located at the center of the picture, and the bridge is oriented with its long axis horizontal. There is some asymmetry in the picture from left to right, and this is due to a phonon drag signal which is superimposed on the absorption: Phonons incident from large angles have a significant momentum component along the line joining the device contacts. This is transferred to the holes in hole-phonon collisions, and the holes are dragged toward one of the contacts, giving rise to a voltage signal which is present even in the absence of a bias current (the drag effect in 2D hole gases is described in more detail in Ref. 28). In order to minimize this drag effect in the other parts of the experiment, the fixed heaters were fabricated along a line running through the center of the bridge and perpendicular to its length. An interesting property of the image is the weakness of any of the

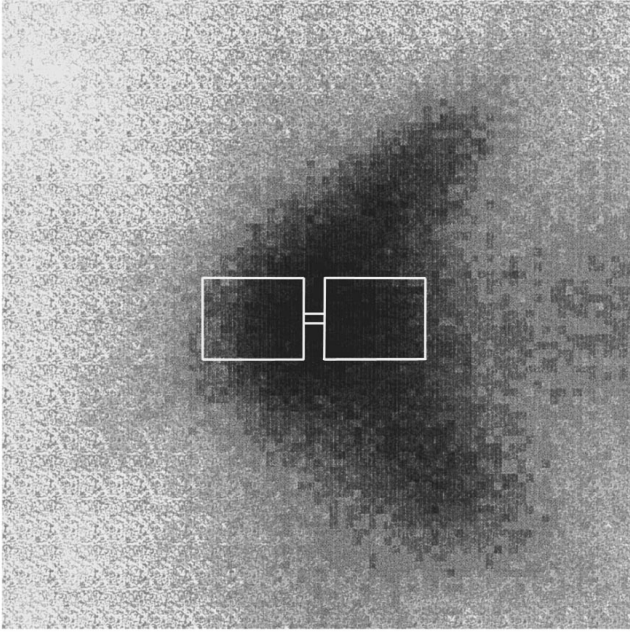


FIG. 10. 2D image of the phonon absorption (both modes). The scan covers an area of  $4 \times 4 \text{ mm}^2$  with the device at its center on the opposite side of the 2-mm wafer.

characteristic features associated with the strong focusing of slow and fast transverse modes in certain directions in cubic symmetry crystals,<sup>29</sup> except perhaps at its very center. This is probably because transverse phonons are only effectively absorbed if they are traveling in a small range of angles ( $< 20^\circ$ ) close to the normal (Fig. 3), while at larger angles the LA mode is dominant and this is only weakly focused.

### B. $B \neq 0$

Figure 11 shows the phonoconductivity signal as a function of magnetic-field strength. The heater temperature in

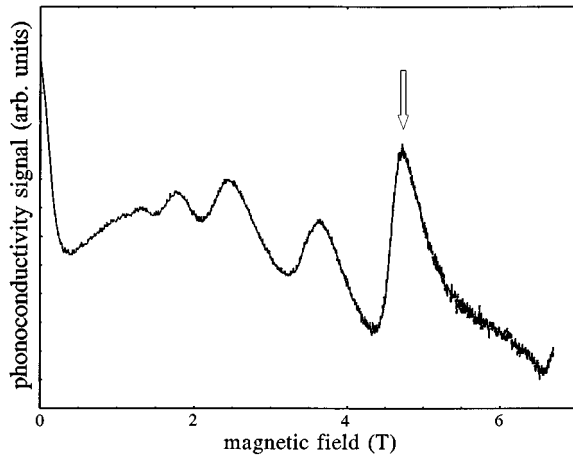


FIG. 11. Intensity of phonon absorption signal as a function of magnetic field applied perpendicular to the plane of the 2DHG. The arrow indicates a peak due to phonon induced inter-Landau-level transitions at  $B = 4.77 \text{ T}$  ( $\nu = 3$ ).

this case was 13 K, corresponding to a phonon frequency of 810 GHz at the peak of the black-body spectral distribution. After an initial decrease, large oscillations in the signal amplitude are seen. Both the strength of the phonon absorption by the 2DHG and the temperature dependence of its conductance are expected to oscillate with the applied magnetic-field strength; however, in this case we believe that the former is dominating the sample response for the following reason: If we assume that the magnitude of the temperature change caused by phonon absorption is about the same as that measured at zero field, and is also constant with changing magnetic field, then we would expect the maxima in the oscillations to occur when the Fermi energy coincides with the Landau levels. In fact this is not the case except for the peak at 3.6 T. Furthermore, the amplitude of the oscillations is much stronger than we would expect on the basis of measurements of the equilibrium temperature dependence of the amplitude of the Shubnikov–de Haas oscillations.

The oscillations form a more simple series than is normally observed in transport measurements on hole gases.<sup>13</sup> This, we believe, is because the phonoconductivity oscillations are dominated by one type of carrier, that is the heavy holes which absorb phonons more strongly. Assuming this to be the case, we can deduce from their positions that all of the peaks except the one at 3.6 T are due to cyclotron frequency phonon absorption. The cyclotron frequency range corresponding to the range of heavy-hole masses found in the literature is  $47B - 117B$  GHz, so even at the highest field/lowest mass the cyclotron frequency is less than the peak phonon frequency. Intralevel transitions contribute to the nonzero background signal.

If the peaks are due to cyclotron phonon absorption the signal strength is expected to be proportional to the number of phonons in the heater spectrum at a single frequency,  $\omega_c$ , i.e.,

$$S(T_s) \propto \frac{1}{\exp\left(\frac{\hbar \omega_c}{kT_s}\right) - 1}.$$

By fitting this function to a plot of signal size as a function of heater temperature,  $T_s$ , shown in Fig. 12, we can extract the cyclotron frequency for the 4.77-T peak indicated by the arrow in Fig. 11. We obtain  $\omega_c/2\pi = 342$  GHz, which implies a heavy-hole effective mass of  $(0.39 \pm 0.05)m_0$ . This figure is in the middle of the range of values obtained from Shubnikov–de Haas measurements,<sup>13</sup> and at the bottom end of the range obtained by conventional cyclotron resonance measurements.<sup>12</sup>

A 2D image of the phonoconductivity at 4.77 T was made using a large area  $3 \times 1\text{-mm}^2$  device on NU899. It showed a uniform bulk response over the whole device area instead of the edge response seen using a 2DEG structure<sup>3</sup> (this reference also gives more details of the imaging technique used). The reason for the difference is that while in the case of the 2DEG the form-factor cutoff occurred at a phonon frequency well below  $\omega_c$ , thus preventing inter-Landau-level transitions in the bulk, for the 2DHG  $a_0$  is smaller and the effective mass much higher, so the cutoff frequency,  $\approx 900$  GHz, is well above the cyclotron frequency.

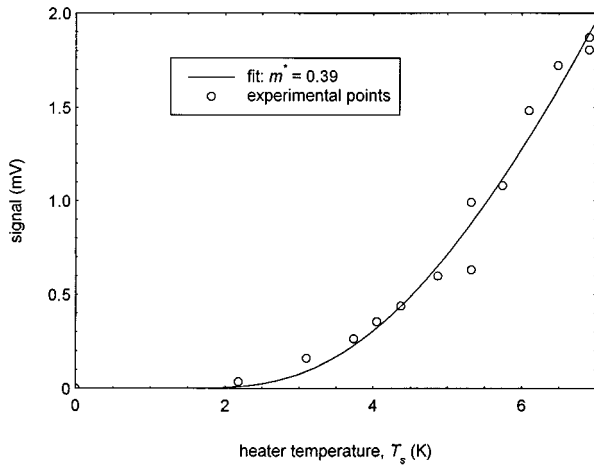


FIG. 12. Phonon absorption signal as a function of heater temperature for the 4.77-T peak in Fig. 11. The solid line is a theoretical fit assuming absorption at  $\omega_c$  and  $m^*=0.39$ .

The question still remains as to what is the cause of the peak at 3.6 T. At this field  $E_F$  is coincident with a Landau level, so the most obvious possibility is that this peak is due to low-frequency absorption and intralevel transitions. However, the peak is surprisingly strong compared to the rest, considering that it would be due to the absorption of a rather narrow band of low-frequency phonons. Furthermore, the peak amplitude would be expected to have a different heater temperature dependence to the one at 4.77 T. In fact, it was possible to fit the above form for  $S(T_s)$  to the peak height and obtain a value of  $\omega_c/2\pi=520$  GHz which is about twice that expected at 3.6 T using  $m^*=0.39m_0$ . It is inconceivable that the effective mass will have halved on changing the field from 4.77 to 3.6 T, we therefore attribute this peak to a  $2\omega_c$  transition.

## V. SUMMARY AND CONCLUSIONS

We have made detailed experimental measurements of the phonon absorption by a 2D hole gas in a GaAs heterojunction in zero and applied magnetic fields. We have used the results to test a simple theory of the phonon absorption at low temperatures and hole densities, which is developed from the theory of 2DEG-phonon interactions, with the adoption of the appropriate values of the hole effective mass and the effective valance-band deformation potential. We found that this theory gives a good quantitative description of all the main features of the phonon absorption, including the mode and wave-vector dependencies, without recourse to considering the complicated details of the hole subband structure. This work provides added justification for the use of such a theoretical approach in straightforward calculations of the low-temperature transport properties of a 2DHG.

At the temperatures used in the experiments, the absorption is dominated by deformation potential coupling to the heavy holes in the spin-split lowest subband. The strength of the fractional absorption is of order  $10^{-6}\%$ , and depends on the angle of incidence of the phonons, being stronger for near to normal incidence.

We were able to determine the Fang-Howard parameter for the hole gas which is in the range 1.0–1.4 nm depending on hole density. We also obtained the heavy-hole effective mass,  $m^*=(0.39\pm 0.05)m_0$ , using a ‘‘phonon cyclotron resonance’’ measurement.

## ACKNOWLEDGMENTS

We would like to thank the following for helpful discussions and comments: Dr. D Lehmann, Dr. Cz Jasiukiewicz, and Dr. P. Hawker. This work was supported by grants from the UK Engineering and Physical Sciences Research Council, and the European Union.

- <sup>1</sup>L. J. Challis and A. J. Kent, in *Physics of Phonons, Proceedings of the 29th Winter School on Theoretical Physics*, edited by T. Paszkiewicz and K. Rapcewicz (Plenum, New York, 1994), p. 1159.
- <sup>2</sup>A. J. Kent, G. A. Hardy, P. Hawker, V. W. Rampton, M. I. Newton, P. A. Russell, and L. J. Challis, *Phys. Rev. Lett.* **61**, 180 (1988).
- <sup>3</sup>D. J. McKitterick, A. Shik, A. J. Kent, and M. Henini, *Phys. Rev. B* **49**, 2585 (1994).
- <sup>4</sup>C. J. Mellor, R. H. Eyles, J. E. Digby, A. J. Kent, K. A. Benedict, L. J. Challis, M. Henini, C. T. Foxon, and J. J. Harris, *Phys. Rev. Lett.* **74**, 2339 (1995).
- <sup>5</sup>M. A. Chin, V. Narayanamurti, H. L. Stormer, and A. C. Gossard, in *Proceedings of the 17th International Conference on the Physics of Semiconductors*, edited by J. D. Cahdi and W. A. Harrison (Springer, Berlin, 1985), p. 333.
- <sup>6</sup>A. J. Kent, K. R. Strickland, and M. Henini, in *Phonon Scattering in Condensed Matter VII*, edited by M. Meissner and R. O. Pohl (Springer, Berlin, 1993), p. 359.

- <sup>7</sup>K. R. Strickland, R. E. George, M. Henini, and A. J. Kent, *Semicond. Sci. Technol.* **9**, 786 (1994).
- <sup>8</sup>E. E. Mendez and W. I. Wang, *Appl. Phys. Lett.* **46**, 1159 (1985).
- <sup>9</sup>U. Ekenberg and M. Altarelli, *Phys. Rev. B* **30**, 3569 (1984).
- <sup>10</sup>W. Walukiewicz, *Phys. Rev. B* **31**, 5557 (1985).
- <sup>11</sup>D. A. Broido and L. J. Sham, *Phys. Rev. B* **31**, 888 (1985).
- <sup>12</sup>H. L. Stormer, Z. Schlesinger, A. Chang, D. C. Tsui, A. C. Gossard, and W. Wiegmann, *Phys. Rev. Lett.* **51**, 126 (1983).
- <sup>13</sup>E. E. Mendez, *Surf. Sci.* **170**, 561 (1986).
- <sup>14</sup>G. E. Pikus and G. L. Bir, *Fiz. Tverd. Tela (Leningrad)* **1**, 1642 (1959) [*Sov. Phys. Solid State* **1**, 1502 (1960)].
- <sup>15</sup>G. L. Bir and G. E. Pikus, *Fiz. Tverd. Tela (Leningrad)* **2**, 2287 (1960) [*Sov. Phys. Solid State* **2**, 2039 (1961)].
- <sup>16</sup>J. D. Wiley, in *Transport Phenomena*, edited by R. K. Willardson and A. C. Beer, *Semiconductors and Semimetals Vol. 10* (Academic, New York, 1975), Chap. 2.
- <sup>17</sup>J. C. Hensel, B. I. Halperin, and R. C. Dynes, *Phys. Rev. Lett.* **44**, 341 (1980).
- <sup>18</sup>J. C. Hensel, R. C. Dynes, and D. C. Tsui, *Phys. Rev. B* **28**, 1124 (1983).



- <sup>19</sup>F. F. Fang and W. E. Howard, Phys. Rev. Lett. **16**, 797 (1966).
- <sup>20</sup>W. Walukiewicz, Phys. Rev. B **37**, 8530 (1988).
- <sup>21</sup>S. Adachi, J. Appl. Phys. **58**, R1 (1985).
- <sup>22</sup>G. A. Toombs, F. W. Sheard, D. Neilson, and L. J. Challis, Solid State Commun. **64**, 577 (1987).
- <sup>23</sup>H. A. J. M. Reinen, T. T. J. M. Berendschot, R. J. H. Kappert, and H. J. A. Bluysen, Solid State Commun. **65**, 1495 (1988).
- <sup>24</sup>K. A. Benedict, J. Phys. Condensed Matter **4**, 4083 (1992).
- <sup>25</sup>F. Rosch and O. Weis, Z. Phys. B **27**, 33 (1977).
- <sup>26</sup>A. J. Kent, Physica B **169**, 356 (1991).
- <sup>27</sup>W. Gańcza and T. Paszkiewicz, Comput. Phys. Commun. **85**, 423 (1995).
- <sup>28</sup>W. Gańcza, Cz. Jasiukiewicz, A. J. Kent, D. Lehmann, T. Paszkiewicz, K. R. Strickland, and R. E. Strickland, Semicond. Sci. Technol. (to be published).
- <sup>29</sup>See, for example, G. A. Northrop and J. P. Wolfe, in *Nonequilibrium Phonon Dynamics*, Vol. 124 of *NATO Advanced Study Institute Series B. Physics*, edited by W. E. Bron (Plenum, New York, 1985), p. 185.